Langmuir

ARTICLE

pubs.acs.org/Langmuir

$NaBH_4$-Induced Assembly of Immobilized Au Nanoparticles into Chainlike Structures on a Chemically Modified Glass Surface

Zhiqiang Zhang[†] and Yihui Wu*[,†,‡]

[†]Suzhou Institute of Biomedical Engineering and Technology, Chinese Academy of Sciences, Suzhou 215163, PR China

[‡]State Key Laboratory of Applied Optics, Changchun Institute of Optics, Fine Mechanics and Physics, Chinese Academy of Sciences, Changchun 130033, PR China

Supporting Information

ABSTRACT: A facile method of obtaining chainlike assemblies of gold nanoparticles (AuNPs) on a chemically modified glass surface based on $NaBH_4$ treatment is developed. Citrate-stabilized AuNPs (17 nm) are immobilized on a glutaraldehyde-functionalized glass surface and assembled into chainlike structures after treatment with aqueous sodium borohydride ($NaBH_4$) solution. The production and morphology of the AuNP chainlike assemblies are controlled by the density of the immobilized NPs, the concentration of $NaBH_4$ solution, and the treatment time. The AuNP assemblies are stable in water and can undergo drying. X-ray photoelectron spectroscopic data show that the number of citrate ions on the AuNPs decreased by 43% after treatment with 5 mg/mL $NaBH_4$ solution. The $NaBH_4$-induced partial removal of the citrate ions and the roughness of the glass surface greatly affect the binding force of AuNPs on the substrate. The immobilized AuNPs begin to move at the solid−liquid interface without desorbing when the strength of the binding force was decreased. These mobile NPs form chainlike assemblies under the driving force of van der Waals interaction and diffusion. This interface-based formation of chainlike assemblies of AuNPs may provide a simple protocol for the 1D assembly of other Au-coated colloidal nanoparticles.

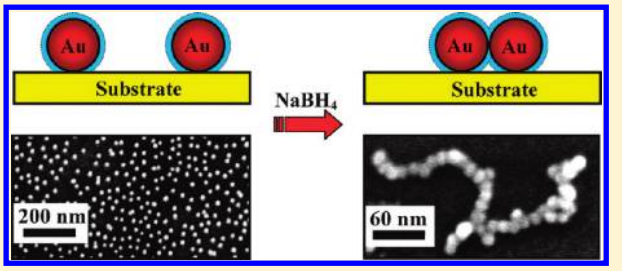

INTRODUCTION

Nanoparticles (NPs) have been used as building blocks for constructing 1D, 2D, and 3D nanostructures with unique electrical, optical, magnetic, and chemical properties.[1] The 1D assembly of gold nanoparticles (AuNPs) has attracted considerable attention because of its potential applications in fabricating nanodevices for electronics, optoelectronics, and sensors. The organization of single NPs into 1D assemblies can be achieved via two main routes,[2] namely, the linear template method, which involves soft and hard templates, and the template-free self-assembly method. The essential point in the integration of NPs into multidimensional assemblies or the desired structures is to create anisotropic properties in the system.[3] This anisotropy can result from specific template morphologies for guided assembly or from the anisotropic interactions between NPs that originate from the intrinsic dipole moment[4] or are induced by anisotropic ligand chemistry.[5]

From another point of view, the self-assembly of NPs into designed nanostructures is, in fact, achieved by constraining the degrees of freedom of these mobile NPs in certain directions and confining them to form specific assemblies. For example, 2D assemblies of NPs have been produced at the liquid−liquid,[6] liquid−gas,[7] solid−liquid,[8] and solid−gas interfaces[9] in which the mobile NPs were constrained to soft or hard interfaces that act as the templates to delete one degree of freedom. Another clear example is the linear template that induces the 1D self-assembly of NPs, where two degrees of freedom are deleted by the dimensions of the template. For template-free self-assembly, however, a solution-based 1D assembly would be difficult because the confinement of the NPs from 3D to 1D requires greater effort to constrain their mobility in the other two dimensions using ligand chemistry. If the degrees of freedom were first reduced from 3D to 2D, then the low dimensional assembly of NPs would become easier. This possibility has been realized by Li et al.,[10] who found that a large-scale 1D chainlike network of AuNPs can be produced at an oil/water interface. In contrast, Mann et al.[11] reported that 1D branched-chain networks of AuNPs were formed in solution by modifying the ligand composition of the NPs. However, the production and dimensions of the network were smaller than those obtained using the former method. Therefore, the interface-based confinement of NPs for 2D assembly may be an efficient approach to 1D assembly.

Previous studies have shown that colloidal AuNPs can be immobilized on chemically functionalized (SH− or NH_2−) substrates through covalent or electrostatic interactions, and the resulting AuNP monolayer has been used as a stable substrate in surface-enhanced Raman scattering (SERS),[12] electrochemistry,[13] and biosensing.[14] However, the degree of freedom of these immobilized AuNPs is reduced to zero because the binding force

Received: May 25, 2011
Revised: July 5, 2011
Published: July 05, 2011

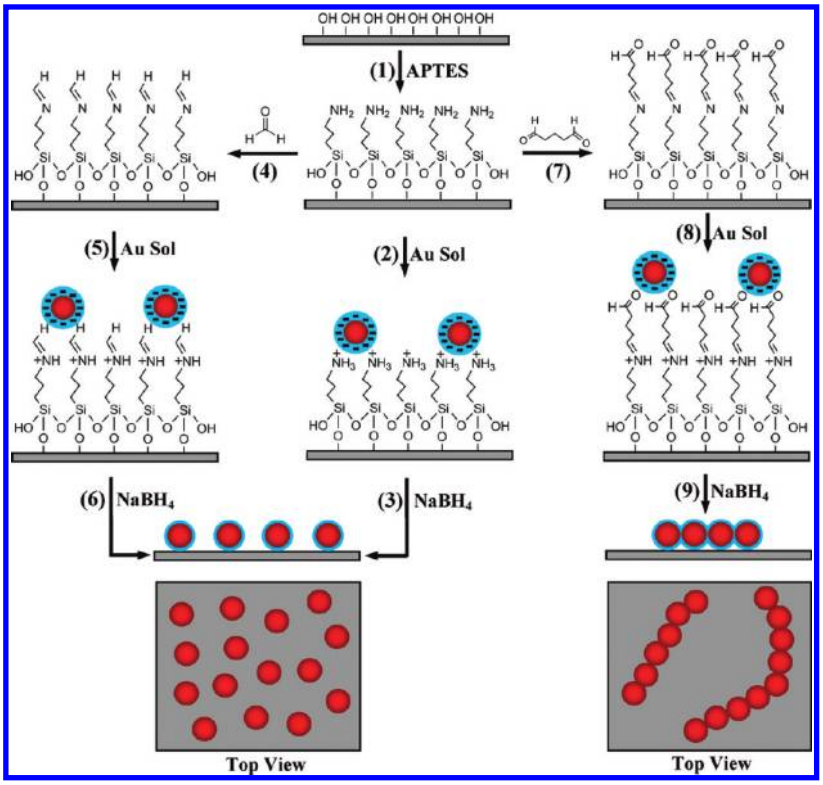

Figure 1. Schematic diagram of the chemical modification of the glass substrate for the chainlike assembly of 17 nm AuNPs. 1 → 2 → 3: AuNP/NH_2. 1 → 4 → 5 → 6: AuNP/FA/NH_2. 1 → 7 → 8 → 9: AuNP/GA/NH_2.

is strong enough to overcome the thermal diffusion of the NPs. There is a possibility that the NPs may begin to move on the solid surface when the magnitude of the binding force decreases to a certain value and the degrees of freedom of these loosely bound NPs become 2D. Liu et al.[9a] used an AuNP monolayer as a precursor to form an ordered 2D AuNP film based on the evaporation method in which the electrostatic binding force between the NPs and the substrates was greatly weakened because of the encapsulation of the NPs by alkanethiol molecules. The adsorbed alkanethiol layer fully screened the electrical double layer of the NPs and rendered the interaction between the NPs isotropic. Thus, anisotropic interactions between the NPs should be induced to promote the anisotropic assembly of NPs at this interface. Most recently, citrate ions adsorbed onto the surfaces of AuNPs were partially removed after sodium borohydride ($NaBH_4$) treatment, and non-close-packed aggregates of AuNPs were formed in the solution.[15]

In the current study, a facile approach to the controlled assembly of immobilized 17 nm AuNPs into chainlike structures over a large area on a chemically modified glass surface was developed on the basis of $NaBH_4$ treatment. A schematic illustration is shown in Figure 1. Citrate-stabilized AuNPs are immobilized on the glutaraldehyde (GA)-functionalized glass surface that was previously modified with (3-aminopropyl)-triethoxysilane (APTES) and subsequently form an AuNP monolayer. The binding force results from the electrostatic interaction between the negatively charged AuNPs and the positively charged Schiff base. These immobilized AuNPs assemble into chainlike structures after treatment with aqueous $NaBH_4$ solution. The production and morphology of the chainlike assemblies are controlled by parameters such as the NP density on the glass surface and the concentration and treatment time of $NaBH_4$. This interface-based formation of AuNP chainlike assemblies may provide a simple synthesis method for other Au-coated colloidal nanoparticles.

EXPERIMENTAL METHODS

Materials. $NaBH_4$ (≥98%), APTES (99%), and GA (25% in H_2O) were purchased from Aldrich. Hydrogen tetrachloroaurate ($HAuCl_4 \cdot 4H_2O$, >99.9%) and trisodium citrate ($C_6H_5O_7Na_3 \cdot 2H_2O$, ≥99.0%) were purchased from Beijing Chemical Reagents (Beijing, PR China) and used without further purification. Milli-Q H_2O (18.2 $M\Omega \cdot cm^{-1}$) was used for all experiments. All other reagents were of analytical grade.

Synthesis of 17 nm AuNPs. Aqueous suspensions of citrate-stabilized AuNPs were prepared using the Frens method.[16] Briefly, 200 mL of a 0.01% (w/v) $HAuCl_4$ solution was heated to boiling under vigorous stirring with refluxing. After 1 min, 8 mL of 1% (w/v) sodium citrate was rapidly added to the boiling solution, and the mixture was allowed to boil for 20 min. The prepared gold colloids were then cooled to room temperature with constant stirring and stored at 4 °C in a dark bottle. All glassware was rigorously cleaned in aqua regia (3:1 HCl/HNO_3) and rinsed thoroughly with Milli-Q H_2O before use.

Preparation of APTES-Derivatized Substrates. The glass or silicon (Si) slides were cleaned in piranha solution (7:3 H_2SO_4/H_2O_2) at 120 °C for 20 min, rinsed thoroughly with distilled water, and dried using a flow of pure N_2, in accordance with a previous method.[17] (***Caution!*** *Piranha solution is very corrosive and must be handled with extreme care.*) After being rinsed with methanol for 5 min, the substrates were immersed in 5% (v/v) APTES in methanol for 1 h and rinsed five times in methanol for 10 min, followed by deionized water to hydrolyze the residual ethoxy functionalities for 30 min. The slides were then dried

dx.doi.org/10.1021/la201943u |*Langmuir* 2011, 27, 9834–9842

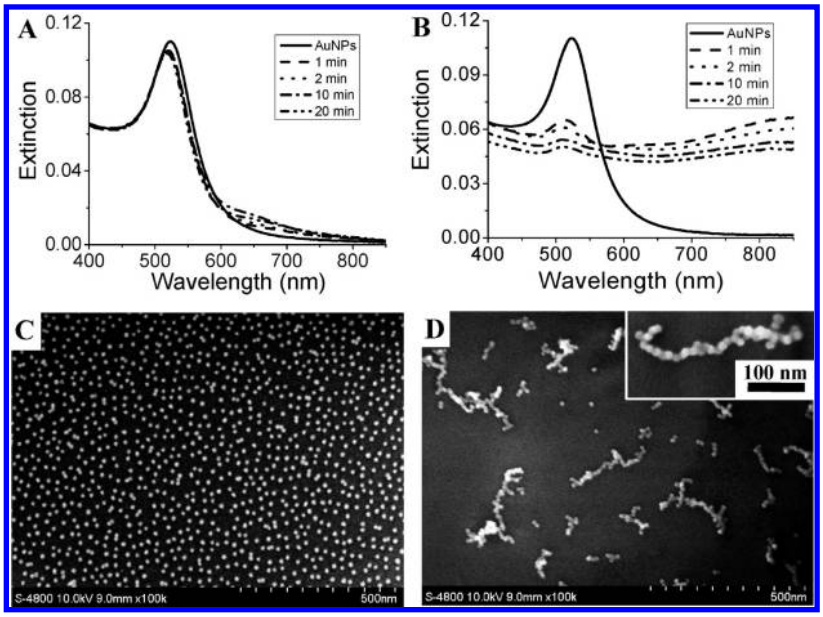

Figure 2. UV/vis extinction spectra of 5 mg/mL $NaBH_4$-treated substrates within 20 min: (A) AuNP/NH_2/glass and (B) AuNP/GA/NH_2/glass. (C, D) SEM images of A and B, respectively, after $NaBH_4$ treatment.

using a flow of pure N_2 at 120 °C for 1 h to promote silane cross-linkage. The APTES-derivatized glass or Si slides (designated as NH_2/SiO_2) were stored in a desiccator for further use.

$NaBH_4$ Treatment of the AuNP Submonolayer. The NH_2/SiO_2 substrates were first treated with a 2.5% GA or 1% aqueous formaldehyde (FA) solution for 1 h to form CHO-modified substrates ($GA/NH_2/SiO_2$ and $FA/NH_2/SiO_2$, respectively). These chemically modified substrates were immersed in AuNP solutions for 12 h to form AuNP submonolayers and then rinsed with Milli-Q H_2O to remove the unbound AuNPs. The AuNP monolayer was immersed in a 5 mg/mL $NaBH_4$ (0.23 M) solution for 20 min, followed by rinsing with Milli-Q water, and then dried in air to investigate the effects of $NaBH_4$ on the citrate ions adsorbed onto the AuNPs. The substrates were immersed in 5 mg/mL $NaBH_4$ for 0.5, 1, 5, 10, and 20 min to investigate the effects of $NaBH_4$ treatment time on AuNP aggregation. The AuNP substrates were immersed in 0.5, 1, 5, and 10 mg/mL $NaBH_4$ solution for 5 min, followed by rinsing with deionized water to determine the effects of $NaBH_4$ concentration on AuNP aggregation. The AuNP substrates were immersed in NaOH solutions at pH 12 and 13.6 for 10 min, followed by rinsing with deionized water to investigate the effects of pH on AuNP aggregation. The AuNP substrates before and after $NaBH_4$ treatment were immersed in 1, 5, and 10% NaCl solutions for 10 min, followed by rinsing with deionized water to determine the effects of ionic strength on AuNP aggregation.

Characterization Methods. All UV−vis extinction spectra were measured using a Perkin-Elmer Lambda 850 UV/vis spectrophotometer. The morphologies of the NP assemblies formed were characterized using a Hitachi S-4800 field-emission scanning electron microscope (FE-SEM). The surface roughness of the glass and Si substrates was characterized using a Nanoscope IIIa.

RESULTS AND DISCUSSION

Formation of Chainlike Structures by AuNPs Immobilized on a Glass Surface. Figure 2 shows the different results of AuNP/NH_2 and AuNP/GA/NH_2 substrates after treatment with 0.13 M $NaBH_4$. As shown in Figure 2B, the extinction band of AuNP/GA/NH_2 above 550 nm was significantly increased after $NaBH_4$ treatment, which indicates that large aggregates were formed. Moreover, AuNP/GA/NH_2 showed a larger blue shift (12.0 nm) of the extinction peak (λ_{max}) compared with that of AuNP/NH_2 (5.0 nm). The blue shift of λ_{max} could result from the increased free electrons by $NaBH_4$ treatment[18] or the transverse plasmon band of the longer 1D NP chains.[19] However, the AuNPs immobilized on the GA/NH_2-modified glass surface formed chainlike structures after $NaBH_4$ treatment, as shown in Figure 2D. However, the AuNPs immobilized on the APTES-modified substrate retained their submonolayer morphology except for a few AuNP dimers and trimers. Similarly, the AuNPs immobilized on the FA-functionalized APTES surface (AuNP/FA/NH_2) were also stable after $NaBH_4$ treatment, as shown by the slight change in the extinction spectrum (Figure S1). Therefore, GA-functionalized glass is suitable for the formation of AuNP chainlike assemblies under $NaBH_4$ treatment.

The AuNP/GA/NH_2 substrate was used as a model for studying several parameters affecting the morphology of the AuNP chainlike structures. The first parameter is the AuNP density, which is controlled by the immersion time of the GA/NH_2 substrate in the AuNP solution (Figure S2). As shown in Figure 3, the length and the production of the AuNP chainlike assemblies increased as the immobilized AuNP density increased. In addition, the number of immobilized AuNPs before $NaBH_4$ treatment was approximately equal to that after treatment, indicating that no NPs were removed from the substrate during $NaBH_4$ treatment.

The second parameter is the $NaBH_4$ concentration. As shown in Figure 4, only a small fraction of AuNPs formed short linear aggregates at low concentration (0.5 mg/mL). The production of chainlike aggregates increased with the increase in $NaBH_4$ concentration. However, these chainlike assemblies became branched aggregates under a higher $NaBH_4$ concentration (10 mg/mL). All AuNP/GA/NH_2 substrates have the same NP density (Figure S3).

The third parameter is the treatment time with $NaBH_4$ solution. Figure 2B shows that the shape of the AuNP optical spectra changed dramatically after treatment with $NaBH_4$ for 1

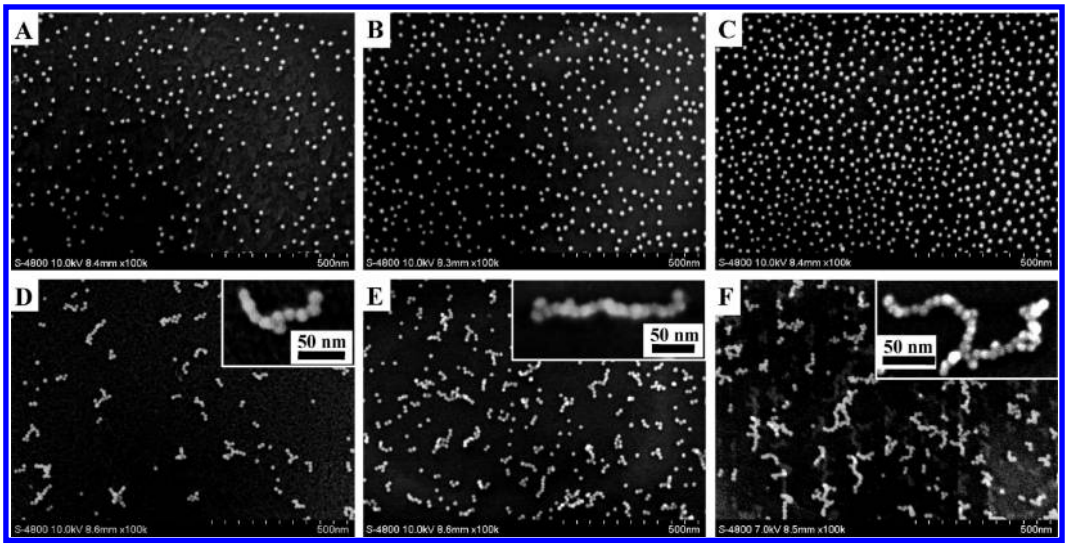

Figure 3. Scanning electron micrographs of AuNP/GA/NH_2 with increased NP density (A−C) before and (D−F) after treatment with 5 mg/mL $NaBH_4$ for 5 min.

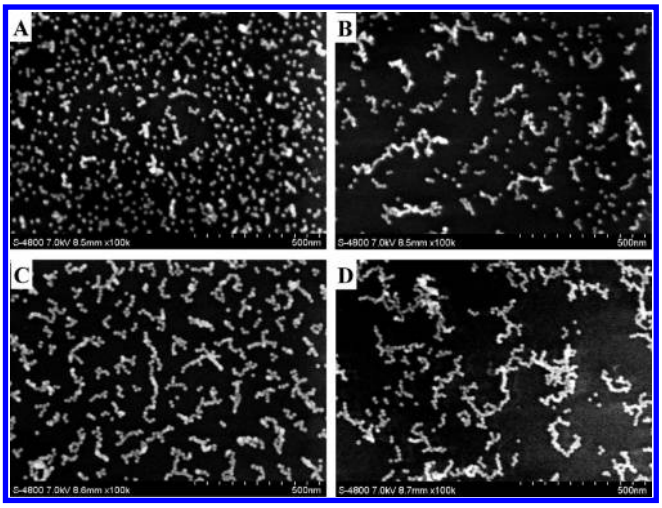

Figure 4. Scanning electron micrographs of AuNP/GA/NH_2 after treatment with different $NaBH_4$ concentrations for 5 min: (A) 0.5, (B) 1, (C) 5, and (D) 10 mg/mL.

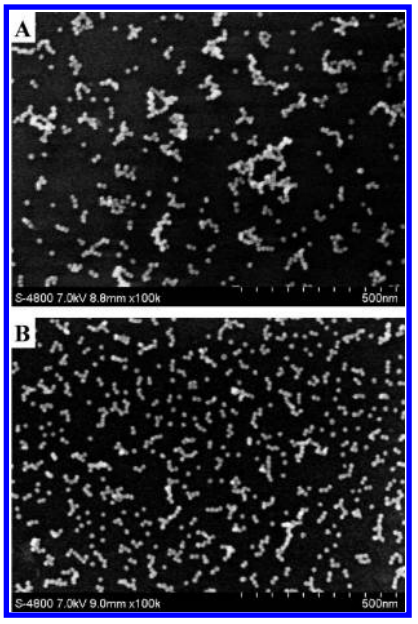

Figure 5. Scanning electron micrographs of AuNP/GA/NH_2 after treatment with 5 mg/mL $NaBH_4$ for (A) 2 s and (B) 1 min.

min; no further significant change was observed within 20 min. This spectrum change was also indirectly observed with the naked eye by the change in the color of the substrates. The red glass substrates (AuNP/GA/NH_2/glass) became gray once they were immersed in the $NaBH_4$ solution (for approximately 2 s) and exhibited no further change with the increase in treatment time, which agrees well with the UV−vis data (Figure S4). The rapid color change of the AuNP substrates can be used as a signal for AuNP aggregation, but it is unsuitable for estimating the formation process of the chainlike aggregates. As shown in Figure 5, the AuNPs treated for 2 s formed large aggregates with branched structures. In contrast, the AuNPs treated for 1 min showed small chainlike aggregates. Therefore, longer $NaBH_4$ treatment times favor the formation of stable AuNP assemblies, which may be due to the greater stability against air drying during sample preparation after $NaBH_4$ treatment.

Stability of the AuNP Chainlike Assemblies. The stability of the NP assemblies produced directly affects the subsequent applications of these assemblies. Two factors that may affect the AuNP assemblies, namely, air drying and storage stability, were considered.

The AuNP substrate treated with $NaBH_4$ for 5 min was dried and wetted three times to study the effects of air drying on the morphology of the chainlike assemblies. As shown in Figure 6, the extinction spectra of both the dried and wetted AuNP substrates coincide well within three circles. The corresponding micrograph shows that the AuNPs still presented chainlike aggregates after being dried three times (Figure S5). Therefore, the air-drying process did not affect the NP structures.

The quickly treated AuNPs formed less-ordered aggregates (Figure 5A) whereas the longer time treated AuNPs formed stable chainlike structures after drying (Figure 6). In the current study, the very short treatment time with $NaBH_4$ resulted in a

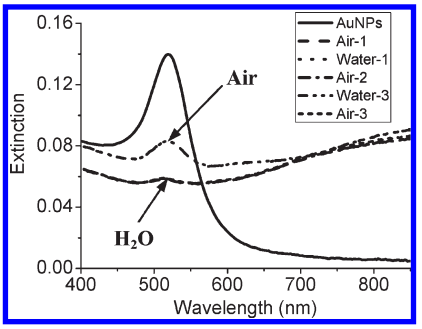

Figure 6. UV/vis extinction spectra of the AuNP/GA/NH_2 substrate after treatment with 5 mg/mL $NaBH_4$ for 5 min, measured in pure water and air three times.

weak bonding force such that the AuNPs could not withstand external disruptions and exhibited instability during the air-drying process. Therefore, the chainlike AuNP structures of the samples obtained after the longer treatment with $NaBH_4$ were induced by the $NaBH_4$ treatment and not by air drying.

The storage stability of the $NaBH_4$-induced chainlike AuNP assemblies was determined using UV−vis spectroscopy in pure water. As shown in Figure 7, the extinction spectra after $NaBH_4$ treatment were identical except for the restoration and the blue shift of λ_{max}, resulting from the discharge and recharge of the AuNPs, respectively, which indicates the good storage stability of the AuNP chainlike structures in water.

Effect of the $NaBH_4$ Treatment on AuNP/GA/NH_2. The results show that the colloidal AuNPs were adsorbed onto the GA-functionalized substrate to form an AuNP submonolayer (Figure 2), and these immobilized NPs formed chainlike aggregates after $NaBH_4$ treatment. The effect of the $NaBH_4$ treatment on AuNP/GA/NH_2 may be influenced by several factors, including the ionic strength and pH of the $NaBH_4$ solution, the oxidation of the Schiff base bond (−C═N) into an imide bond (−C−N), the oxidation of the aldehyde group (−CHO) into a hydroxyl group (−COH), and the partial removal of the citrate ion from the AuNPs.

The stability of the immobilized AuNPs depends on the electrostatic binding force, which is related to the number of negatively charged citrate ions and the protonated N atoms in the contact region. However, both AuNP/GA/NH_2 and AuNP/NH_2 exhibited good stability under high ionic strengths (Figure S6) and basic solutions with much higher pH values (pH 12) than for the $NaBH_4$ solution (ca. pH 10 at 10 mg/mL) (Figure S7). Therefore, the first effect alone does not affect the binding force of the AuNPs. In particular, the high pH does not significantly affect the protonation of the N atoms in the Schiff base bond, which may be attributed to the condensed self-assembled monolayers (SAMs) of the chemical layer (GA/NH_2). Therefore, the second effect of $NaBH_4$ should not influence the immobilized AuNPs except for a few exposed Schiff base bonds that resulted from the imperfectly formed SAMs.

In our previous study,[15] a small quantity of citrate ions (33%) were removed from the AuNP surface after $NaBH_4$ treatment (6 mM). However, the concentration of the $NaBH_4$ solution used in the current work was much higher than that used in the previous study. AuNP/NH_2/Si was used as a substrate for $NaBH_4$ treatment, and XPS was utilized to quantify the citrate molecule removal induced by 0.13 M $NaBH_4$ solution. As shown in Figure 8, the densities of the AuNPs immobilized on the NH_2/

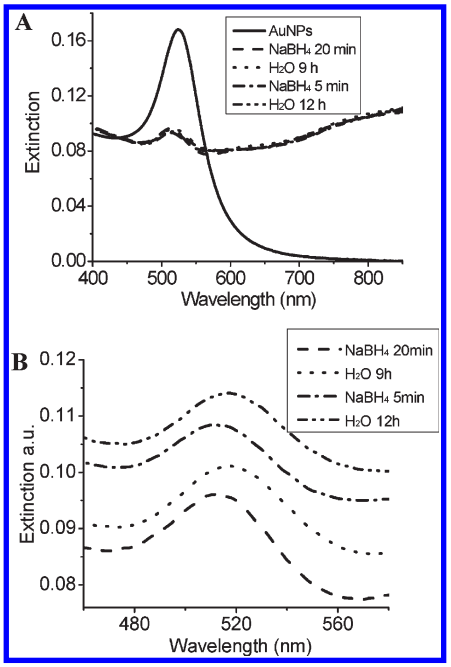

Figure 7. UV/vis extinction spectra of AuNP/GA/NH_2 treated with 5 mg/mL $NaBH_4$.

Si wafer before and after treatment with 0.13 M $NaBH_4$ are the same, and the COO^- component, which represents citrate, decreased by 43% after the $NaBH_4$ treatment.

The distinct responses of AuNP/GA/NH_2 and AuNP/NH_2 with the same number of citrate ions removed indicate the different effects of $NaBH_4$ on their binding forces. For AuNP/NH_2, the binding force was strong enough to hold the NPs on the substrate because the citrate ions in the contact region may not have been affected by $NaBH_4$ as a result of the zero gap between the AuNPs and the APTES layer (Figure 9a) or because a new binding force may have formed when the electrostatic binding force disappeared when the citrate ions in the contact region were removed by $NaBH_4$ (Figure 9b). The latter possibility could originate from the Au−N bond, whose strength is that between Au−S and Au−COOH.[20]

For AuNP/GA/NH_2, the binding force was generated from the negatively charged citrate ions and the positively charged N atoms in the Schiff base bond. However, the distance between the counterions is much longer than that in AuNP/NH_2, which results in a weaker binding force compared to the latter. This binding force can easily disappear, and it can result in the desorption of the AuNPs from the substrate if the citrate ions are removed from the AuNPs. However, the AuNPs immobilized on the GA/NH_2 surface still remained after $NaBH_4$ treatment, indicating that a certain binding force inhibited the desorption of AuNPs from the surface. The Au−N bond force may have acted as the new binding force. However, this possibility seems to be contradictory to the ideal GA/NH_2 SAMs because the N atoms are far from the top of the SAMs and thus cannot contribute to the Au−N bond. In fact, the quality of the SAMs on one substrate is determined by the surface quality of the substrate.[21] For the glass slide, the morphology of the APTES-functionalized substrate shows a much greater roughness compared to that of the APTES-modified Si wafer substrates (Figure 10D,F). In this case, the possibility of a reaction between the exposed N atoms of the Schiff base bond and the exposed part of the

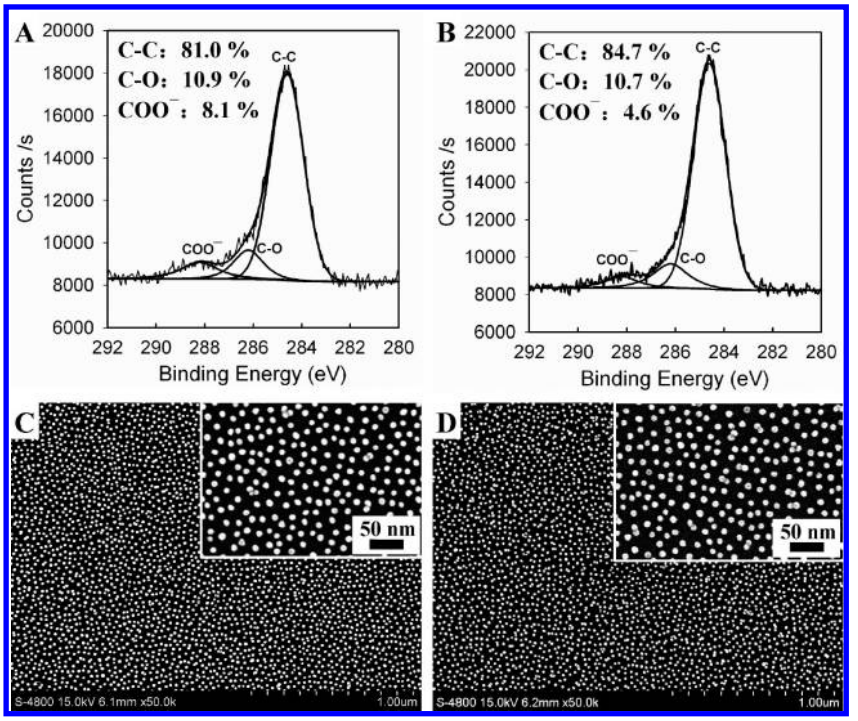

Figure 8. Deconvolved XPS spectra of the C 1s region of the AuNP/NH_2/Si substrates (A) before and (B) after treatment with 5 mg/mL $NaBH_4$ for 20 min and (C, D) the corresponding scanning electron micrographs.

AuNPs, resulting from the poor roughness of the glass surface, would be increased, and eventually the number of Au−N bonds would increase and would generate a new binding force. Therefore, the third effect of $NaBH_4$ plays a significant role in the formation of the AuNP chainlike aggregates.

Effect of the Substrate Roughness on the Binding Force. A polished Si wafer with good surface quality was used for comparison to investigate the effects of substrate roughness on $NaBH_4$-induced AuNP assembly. The AuNPs immobilized on the chemically functionalized Si wafer substrate (AuNP/GA/NH_2/Si) did not form chainlike assemblies after $NaBH_4$ treatment but showed some small irregular aggregates (Figure 11). This notable difference between the Si and glass substrates can be explained by the effect of roughness (Figure 12), according to their section morphologies in the AFM data (Figure S8).

For a smooth surface (low roughness), the chemically modified APTES layer should be more ordered and denser than a rough surface (high roughness).[21] Therefore, for low-roughness surfaces, the contact region between the AuNPs and the APTES layer or the binding force cannot be largely affected by $NaBH_4$ because of the ordered self-assembly of the APTES monolayer, which explains why the AuNPs immobilized on the Si wafer surface did not aggregate. In contrast, the binding force between the AuNPs and the glass surface can be easily affected by $NaBH_4$ treatment because of the small contact region and the disordered APTES/GA monolayer.

The APTES layer on the Si wafer surface after GA modification shows a number of tiny convex peaks (Figure 10B,E). This subtle change after GA functionalization may be due to the quality of GA itself because the GA molecules in the stock solution can undergo self-polymerization, which can be confirmed by the extinction band at 288 nm.[22] Therefore, the AuNPs

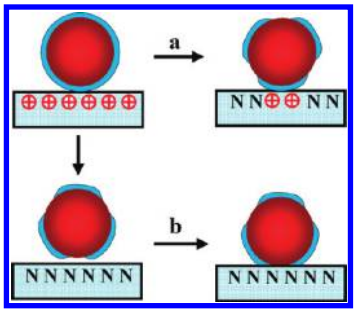

Figure 9. Scheme of the two possible reasons for the stability of AuNP/NH_2 after $NaBH_4$ treatment.

immobilized on this nonideal GA/APTES layer on a smooth surface have a greater likelihood of being affected by $NaBH_4$ than on the ideal GA/APTES layer.

Mechanism of AuNP Chainlike Assembly. The aforementioned discussions have elucidated how the immobilized AuNPs on the chemically modified glass substrate can move without desorption when treated with $NaBH_4$. Why did these mobile AuNPs with 2D degrees of freedom form 1D chainlike structures but not 2D or fractal aggregates? From the interaction analysis of the immobilized AuNPs (Figure 13), the NPs begin to move on the solid−liquid interface without desorbing only when the strength of the binding force (F1) decreases to a certain value, where the interactions between the NPs (F2) and the Brown diffusion (F3) becomes the dominant force that drives the movement of NPs. However, the ionic strength of the $NaBH_4$ solution used was high enough to screen the electrostatic repulsion between the NPs, as shown in Figure 14A. In this case, the driving force is actually composed of the van der Waals attraction and diffusion.

dx.doi.org/10.1021/la201943u |*Langmuir* 2011, 27, 9834–9842

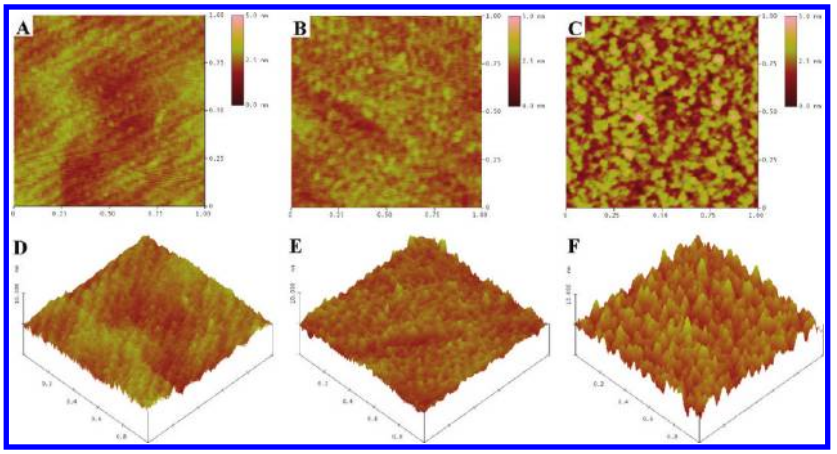

Figure 10. Atomic force micrographs of (A, D) APTES/Si, (B, E) GA/APTES/Si, and (C, F) APTES/glass.

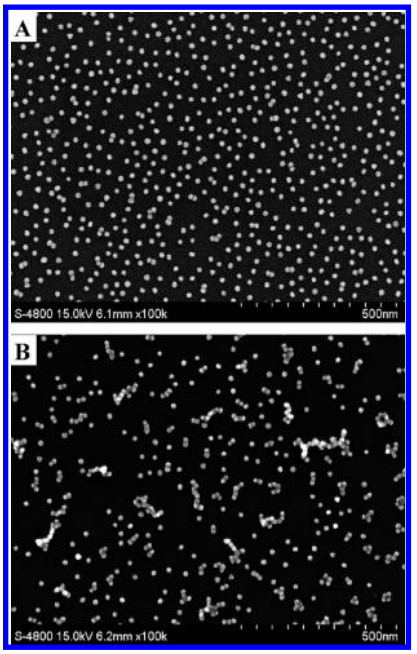

Figure 11. Scanning electron micrographs of AuNP/GA/NH_2/Si (A) before and (B) after treatment with 5 mg/mL $NaBH_4$ for 5 min.

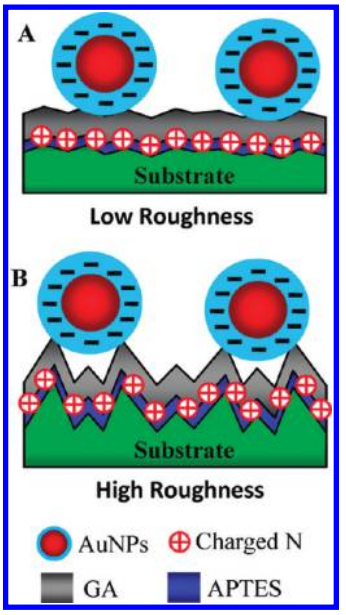

Figure 12. Schematic diagram illustrating the effect of substrate roughness on AuNP/GA/NH_2/substrate: (A) a low-roughness substrate and (B) a high-roughness substrate.

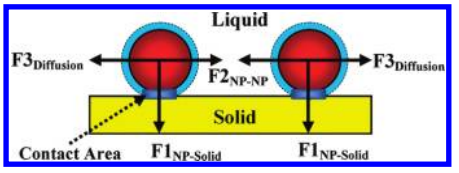

Figure 13. Scheme of the interaction analysis of the AuNPs immobilized on a solid substrate.

Under the driving force, the mobile AuNPs can form chainlike assemblies via three possible mechanisms. The first one is based on the diffusion-limited aggregation model (DLA)[23] in which the freely moving NPs on a 2D plane preferentially form fractal aggregates. However, the immobilized AuNPs on the GA/APTES surface still have a weak binding force (Au−N bond) after $NaBH_4$ treatment. This new binding force decreases the speed of formation of the fractal aggregates until finally only pieces of fractal aggregates are formed. The colored chainlike assemblies of structure P1 in Figure 14B are one example.

Another possible mechanism is the $NaBH_4$-induced anisotropic interactions between AuNPs. The high concentration of the $NaBH_4$ solution not only induces the partial removal of the citrate ions from the AuNPs but also screens the electrical double layer because of its ionic strength. The high concentration of Na^+ in the solution may reverse the charge sign of the NPs because of the high density of counterions or may induce some non-DLVO effects.[24] These two effects of Na^+ affect only the residual citrate ions on AuNPs with an anisotropic distribution. Therefore, anisotropic interactions between NPs can be generated and chainlike aggregates of AuNPs can be formed (structure P2 in Figure 14B).

The third one is based on the shape-selective assembly of NPs.[25] Previous studies[26] have suggested that the solution-phase synthesis of metallic NPs usually contains various morphologies, such as decahedrons, tetrahedrons, truncated tetrahedrons, and cubes. When the third NP comes close to the NP dimer, it

dx.doi.org/10.1021/la201943u |*Langmuir* 2011, 27, 9834–9842

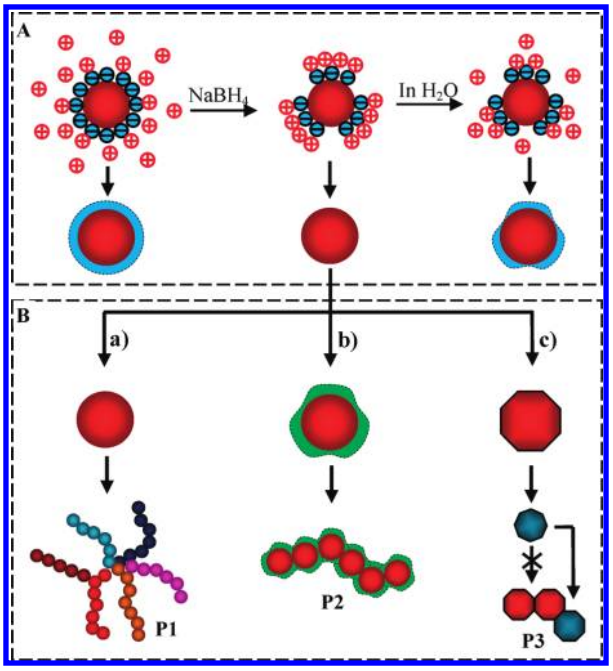

Figure 14. Scheme of the mechanism of AuNP chainlike assembly induced by $NaBH_4$. (A) $NaBH_4$-induced removal of citrate ions. (B) Three possible means of AuNP chainlike assembly: (a) limited-diffusion aggregation, (b) anisotropic interactions generated by $NaBH_4$, and (c) shape-selective assembly of NPs.

preferentially assembles along the transverse direction of former assemblies because of larger steric constraints along the longitudinal direction (structure P3 in Figure 14B).

CONCLUSIONS

A facile approach to the $NaBH_4$-induced assembly of immobilized AuNPs into chainlike structures on a chemically modified glass surface is demonstrated. Citrate-stabilized AuNPs were immobilized on a GA-functionalized glass surface and assembled into chainlike structures after $NaBH_4$ treatment. The binding force of AuNPs on the substrate is affected by the $NaBH_4$-induced partial removal of citrate ions and the roughness of the glass surface. The AuNPs began to move at the solid−liquid interface without desorption when the strength of the binding force decreased. The $NaBH_4$-induced chainlike assembly of AuNPs can be controlled through several parameters, including the NP density, $NaBH_4$ concentration, and treatment time. These mobile NPs formed chainlike assemblies though three possible mechanisms: limited-diffusion aggregation, anisotropic interactions generated by $NaBH_4$, and shape-selective NP assembly. This interface-based assembly of AuNPs is expected to provide a simple protocol for the chainlike assembly of other Au-coated colloidal nanoparticles.

ASSOCIATED CONTENT

Supporting Information. Extinction spectra of the AuNP/FA/NH_2 and AuNP/GA/NH_2 substrates with increased NP density after $NaBH_4$ treatment. Extinction spectra of AuNP/GA/NH_2 substrates after treatment with different concentrations of $NaBH_4$ and NaCl and different $NaBH_4$ treatment times. Extinction spectra of AuNP/GA/NH_2 and AuNP/NH_2 substrates after treatment with aqueous solutions at pH 12 and AFM section morphologies of a chemically modified silicon wafer and glass slide. SEM image of an $NaBH_4$-treated AuNP/GA/NH_2 substrate after being dried and wetted three times. This material is available free of charge via the Internet at http://pubs.acs.org.

AUTHOR INFORMATION

Corresponding Author

*Tel: +86-0431-86176915. Fax: +86-0431-85690271. E-mail: yihuiwu@ciomp.ac.cn.

ACKNOWLEDGMENT

We thank the State Key Program of the National Natural Science Foundation of China (no. 11034007), the General Program of the National Natural Science Foundation of China (no. 60971025), and the Funds of the Chinese Academy of Sciences for Key Topics in Innovation Engineering (no. KJCX2-YW-H18) for financial support.

REFERENCES

(1) (a) Alivisatos, A. P. *Science* **1996**, *271*, 933–937. (b) Murray, C. B.; Kagan, C. R.; Bawendi, M. G. *Annu. Rev. Mater. Sci.* **2000**, *30*, 545–610. (c) Li, F.; Josephson, D. P.; Stein, A. *Angew. Chem., Int. Ed.* **2011**, *50*, 360–388. (d) Katz, E.; Willner, I. *Angew. Chem., Int. Ed.* **2004**, *43*, 6042–6108. (e) Shipway, A. N.; Katz, E.; Willner, I. *ChemPhysChem* **2000**, *1*, 18–52.

(2) Tang, Z.; Kotov, N. A. *Adv. Mater.* **2005**, *17*, 951–962.

(3) Glotzer, S. C.; Solomon, M. J. *Nat. Mater.* **2007**, *6*, 557–562.

(4) Tang, Z.; Kotov, N. A.; Giersig, M. *Science* **2002**, *297*, 237–240.

(5) (a) DeVries, G. A.; Brunnbauer, M.; Hu, Y.; Jackson, A. M.; Long, B.; Neltner, B. T.; Uzun, O.; Wunsch, B. H.; Stellacci, F. *Science* **2007**, *315*, 358–361. (b) Grzelczak, M.; Vermant, J.; Furst, E. M.; Liz-Marzán, L. M. *ACS Nano* **2010**, *4*, 3591–3605.

(6) (a) Duan, H.; Wang, D.; Kurth, D.; Möhwald, H. *Angew. Chem., Int. Ed.* **2004**, *43*, 5639–5642. (b) Su, B.; Abid, J.-P.; Fermín, D. J.; Girault, H. H.; Hoffmannová, H.; Krtil, P.; Samec, Z. *J. Am. Chem. Soc.* **2003**, *126*, 915–919.

(7) (a) Bigioni, T.; Lin, X.; Nguyen, T.; Corwin, E.; Witten, T.; Jaeger, H. *Nat. Mater.* **2006**, *5*, 265–270. (b) Fendler, J. H.; Meldrum, F. C. *Adv. Mater.* **1995**, *7*, 607–632.

(8) (a) Colvin, V. L.; Goldstein, A. N.; Alivisatos, A. P. *J. Am. Chem. Soc.* **1992**, *114*, 5221–5230. (b) Giersig, M.; Mulvaney, P. *Langmuir* **1993**, *9*, 3408–3413. (c) Brown, T.; Johnson, B. *Chem. Commun.* **1997**, *1997*, 1007–1008.

(9) (a) Liu, S.; Zhu, T.; Hu, R.; Liu, Z. *Phys. Chem. Chem. Phys.* **2002**, *4*, 6059–6062. (b) Rabani, E.; Reichman, D.; Geissler, P.; Brus, L. *Nature* **2003**, *426*, 271–274.

(10) Wang, M. H.; Li, Y. J.; Xie, Z. X.; Liu, C.; Yeung, E. S. *Mater. Chem. Phys.* **2010**, *119*, 153–157.

(11) (a) Lin, S.; Li, M.; Dujardin, E.; Girard, C.; Mann, S. *Adv. Mater.* **2005**, *17*, 2553–2559. (b) Li, M.; Johnson, S.; Guo, H.; Dujardin, E.; Mann, S. *Adv. Funct. Mater.* **2011**, *21*, 851–859.

(12) (a) Freeman, R. G.; Grabar, K. C.; Allison, K. J.; Bright, R. M.; Davis, J. A.; Guthrie, A. P.; Hommer, M. B.; Jackson, M. A.; Smith, P. C.; Walter, D. G.; Natan, M. J. *Science* **1995**, *267*, 1629–1632. (b) Chumanov, G.; Sokolov, K.; Gregory, B. W.; Cotton, T. M. *J. Phys. Chem.* **1995**, *99*, 9466–9471.

(13) (a) Doron, A.; Katz, E.; Willner, I. *Langmuir* **1995**, *11*, 1313–1317. (b) Shipway, A.; Lahav, M.; Willner, I. *Adv. Mater.* **2000**, *12*, 993–998.

(14) (a) Frederix, F.; Friedt, J.-M.; Choi, K.-H.; Laureyn, W.; Campitelli, A.; Mondelaers, D.; Maes, G.; Borghs, G. *Anal. Chem.* **2003**, *75*, 6894–6900. (b) Nath, N.; Chilkoti, A. *Anal. Chem.* **2004**, *76*, 5370–5378.

(15) Zhang, Z.; Wu, Y. *Langmuir* **2010**, *26*, 9214–9223.
(16) Frens, G. *Nature* **1973**, *241*, 20–22.
(17) Howarter, J. A.; Youngblood, J. P. *Langmuir* **2006**, *22*, 11142–11147.
(18) (a) Mulvaney, P. *Langmuir* **1996**, *12*, 788–800. (b) Mulvaney, P.; Pérez-Juste, J.; Giersig, M.; Liz-Marzán, L. M.; Pecharromán, C. *Plasmonics* **2006**, *1*, 61–66.
(19) (a) Sawitowski, T.; Miquel, Y.; Heilmann, A.; Schmid, G. *Adv. Funct. Mater.* **2001**, *11*, 435–440. (b) Harris, N.; Arnold, M. D.; Blaber, M. G.; Ford, M. J. *J. Phys. Chem. C* **2009**, *113*, 2784–2791.
(20) Chen, F.; Li, X.; Hihath, J.; Huang, Z.; Tao, N. *J. Am. Chem. Soc.* **2006**, *128*, 15874–15881.
(21) More, S.; Graaf, H.; Baune, M.; Wang, C.; Urisu, T. *Jpn. J. Appl. Phys* **2002**, *41*, 4390–4394.
(22) (a) Rasmussen, K. E.; Albrechtsen, J. *Histochem. Cell Biol.* **1974**, *38*, 19–26. (b) Fahimi, H. D.; Drochmans, P.; Popowski, A. *J. Histochem. Cytochem.* **1968**, *16*, 199–204.
(23) (a) Meakin, P. *Phys. Rev. Lett.* **1983**, *51*, 1119. (b) Saxton, M. J. *Biophys. J.* **1992**, *61*, 119–128. (c) Poon, W. C. K.; Haw, M. D. *Adv. Colloid Interface Sci.* **1997**, *73*, 71–126.
(24) Israelachvili, J. N. *Intermolecular and Surface Forces*, 2 ed., Academic Press: London, 1992.
(25) Mallavajula, R. K.; Archer, L. A. *Angew. Chem., Int. Ed.* **2011**, *50*, 578–580.
(26) (a) Wiley, B.; Sun, Y.; Chen, J.; Cang, H.; Li, Z.-Y.; Li, X.; Xia, Y. *MRS Bull.* **2005**, *30*, 356–361. (b) Wiley, B.; Herricks, T.; Sun, Y.; Xia, Y. *Nano Lett.* **2004**, *4*, 1733–1739.